FREQUENCY RESPONSE CORRECTIONS FOR EDDY CORRELATION SYSTEMS

C. J. MOORE

Institute of Hydrology, Wallingford, Oxon, U.K.

(Received in final form 14 April, 1986)

Abstract. Simplified expressions describing the frequency response of eddy correlation systems due to sensor response, path-length averaging, sensor separation and signal processing are presented. A routine procedure for estimating and correcting for the frequency response loss in flux and variance measurements is discussed and illustrated by application to the Institute of Hydrology's 'Hydra' eddy correlation system.

The results show that flux loss from such a system is typically 5 to 10% for sensible and latent heat flux, but can be much larger for momentum flux and variance measurements in certain conditions.

A microcomputer program is included which, with little modification, can be used for estimating flux loss from other eddy correlation systems with different or additional sensors.

1. Introduction

Technological advance in recent years has allowed many improvements in the design of eddy-correlation systems. This is particularly evident in the development of sonic anemometry for the measurement of wind velocity components, and several new designs have been published (e.g., Campbell and Unsworth, 1979; Larsen *et al.*, 1979; Shuttleworth *et al.*, 1982; Coppin and Taylor, 1983). Similar improvements can be found for sensors measuring atmospheric humidity (e.g., Hyson and Hicks, 1975; Raupach, 1978; Moore, 1983), carbon dioxide concentration (see Ohtaki, 1984) and other atmospheric constituents. Such development has improved the accuracy, speed of response and reliability of turbulence measurements. As a result of physical limitations in sensor size and response, experimental siting and data analysis techniques, however, these measurements will always remain frequency band-limited. Hence systematic errors leading to underestimation of turbulent fluxes and variances must be expected.

For the full potential of the eddy-correlation technique to be realized, e.g., the routine measurement of surface sensible and latent heat fluxes, it is important that the magnitude of these errors can be calculated and hence accounted for in the resulting data. Methods for estimating instrumental errors associated with particular sensors have been available for some time. Silverman (1968), Kaimal *et al.* (1968) and Horst (1973) provide path-length averaging and path-separation corrections for particular sonic anemometer arrangements frequently used in atmospheric turbulence research. Robust and inexpensive propellor anemometers have been more popular for use in eddy correlation systems measuring turbulent heat and momentum fluxes. It has been shown that measurements from these systems generally underestimate the actual fluxes by between 5 and 25% (e.g., Moore, 1976; McNeil and Shuttleworth, 1975; Spittlehouse and Black, 1979). Most, if not all, of these errors can be associated with the response of propellor anemometers and these have been treated at some length in the literature (e.g., Hicks, 1972; McBean, 1972; Garratt, 1975).

However, these error analyses are often presented in a complex form which, although theoretically rigorous, can make practical application a formidable task. This paper describes simplified correction formulae for an eddy-correlation system consisting of wind velocity, temperature and humidity sensors (but which could include others), and which uses a data logging/analysis system to provide measurements of sensible heat, latent heat and momentum flux, and the variances of temperature, humidity, and vertical and horizontal wind velocity. These correction formulae provide good approximations to the original theoretical expressions, but are in forms easily applied to the estimation of errors for particular instrument arrangements. As recent developments in eddy-correlation sensors favour use of the sonic anemometer to measure vertical wind velocity, the corrections presented here are based on this vertical wind velocity sensor.

The correction factors considered here are expressed in terms of the convolution of frequency-dependent response functions with the spectral and co-spectral distribution functions associated with atmospheric turbulent variances and fluxes. For example, the correction, ΔF, of the flux, F, of a quantity with specific density, q, is given by,

$$\frac{\Delta F}{F} = 1 - \frac{\int_0^\infty T_{wq}(n) S_{wq}(n)\,\mathrm{d}n}{\int_0^\infty S_{wq}(n)\,\mathrm{d}n} \tag{1}$$

where T_{wq} is the net system co-spectral transfer function associated with sensors of vertical wind velocity, w, and quantity, q. It is the product of the response functions associated with sensor frequency response, size and separation, and with the data logging system. General descriptions of these are provided in Sections 2 to 5. $S_{wq}(n)$ is the atmospheric co-spectrum of w and q at frequency, n (Hz). Expressions for such spectra and co-spectra are given in Section 6.

Section 7 illustrates how the frequency response functions are combined for a typical system, and together with spectral models these are applied to a specific system, the Hydra (see Shuttleworth *et al.*, 1984), to estimate required frequency response corrections to variance and flux measurements.

2. Sensor Response Functions

2.1. Dynamic Frequency Response

The dynamic frequency response of many sensors can be described by the simple first-order gain function, $G(n)$, given by,

$$G(n) = (1 + [2\pi n\tau]^2)^{-1/2}. \tag{2}$$

The response of most temperature sensors used for atmospheric eddy flux measurements can be described by Equation (2), with the appropriate time constant, τ_T, determined from,

$$\tau_T = \gamma d^2 \frac{\rho_m c_m}{k \, \mathrm{Nu}} , \tag{3}$$

where k is the thermal conductivity of air, and γ is 0.25 for cylindrical or 0.167 for spherical sensors of diameter, d, material density, ρ_m, and specific heat capacity, c_m. For conditions in which fast-response temperature sensors are used, the Nusselt number, Nu, is given by (Duchon, 1963, 1964),

$$\mathrm{Nu} = \begin{cases} 0.24 + 0.56 \, \mathrm{Re}^{0.45} & \text{(cylinders)}, \\ 2.00 + 0.18 \, \mathrm{Re}^{0.67} & \text{(spheres)}, \end{cases} \tag{4}$$

where Re is the Reynold's number. Equation (4) must be modified (see Højstrup *et al.*, 1976) if electrical heating and conductive heat losses are significant.

The dynamic response of cup and propellor anemometers is also given by Equation (2). However, the time constant, τ_u, in this case is dependent on windspeed, and is given by L_u/u where L_u is the response length found from wind tunnel experiments (Hicks, 1972) and u is the wind speed.

2.2. Electronic Filtering

The dynamic response of some sensors cannot be defined easily. The high-frequency limit of sensors such as sonic anemometers is ultimately limited by signal multiplexing or sonic pulse frequencies, or in the case of radiation absorption hydrometers, by the chopping frequency of the radiation beam. In practice, these frequencies are usually very high and it is subsequent electronic filtering which effectively determines the 'dynamic' response of such sensors.

Simple resistor-capacitor (RC) filters with a response function given by Equation (2) (τ = RC) can be used, but these have poor attenuation characteristics. Sharper cut-off low-pass filters are necessary to reduce the amount of aliasing which results from electronic noise often associated with a particular switching frequency. Such filtering is commonly provided by using active voltage-controlled voltage-source (VCVS) circuits which can be designed as Butterworth, Bessel, or Chebychev filters. For example, a single stage VCVS circuit with matched circuit components and an amplifier voltage gain of 1.59 gives a two-pole Butterworth filter with a gain given by

$$G_v(n) = \left[1 + \left(\frac{n}{n_0} \right)^4 \right]^{-1/2} . \tag{5}$$

The cut-off frequency, n_0, is $1/(2\pi \mathrm{RC})$.

3. Sensor Line-Averaging

3.1. Scalar quantities

The effect of measuring an atmospheric scalar variable such as temperature or humidity over a finite path can be described by a spectral transfer function, $T_p(n) = \hat{S}_{\alpha\alpha}(n)/S_{\alpha\alpha}(n)$, where $S_{\alpha\alpha}$ and $\hat{S}_{\alpha\alpha}$ represent actual and measured spectra of quantity α, respectively. The transfer function associated with spatial averaging of turbulent fluctuations of frequency, n (or normalized frequency, $f = np/u$) given an angle, θ, between the wind vector and the averaging path of length, p, is (Silverman, 1968),

$$T_p(f, \theta) = \frac{0.142}{f \sin \theta} \int_{-\infty}^{\infty} \left[1 + \left(\frac{x/\pi f - \cos \theta}{\sin \theta} \right)^2 \right]^{-4/3} \frac{\sin^2 x}{x^2} \, dx. \tag{6}$$

If the averaging path is orientated vertically so that it remains approximately perpendicular to the wind vector regardless of wind direction, then the transfer function reduces to the form given by Gurvich (1962), i.e., Equation (6) with $\theta = 90°$. This

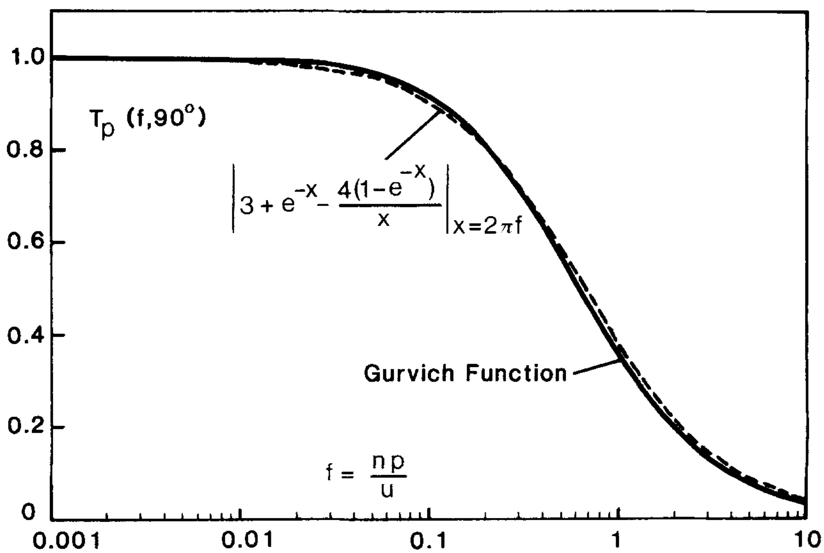

Fig. 1. Spectral transfer function, T_p (f, 90°), associated with the measurement of a scalar quantity averaged over a finite path length, p, at right angles to the horizontal wind velocity, u, and shown as the solid curve plotted against normalized frequency $f = ns/u$. A function approximating this curve is shown as a dashed line.

function is shown in Figure 1. A simplified expression which provides a working description of the Gurvich function to an accuracy of better than 5% for normalized frequencies up to about 10 is also shown in Figure 1, and has the form,

$$T_p(f, 90) = \frac{1}{2\pi f} \left(3 + e^{-2\pi f} - 4 \frac{(1 - e^{-2\pi f})}{2\pi f} \right) . \tag{7}$$

This equation is considered sufficiently accurate for estimating the loss in turbulent flux measurements in most cases. However, an alternate expression must be used if the wind vector exceeds, say, 30° from the perpendicular to the averaging path; for example, if θ is close to zero, the transfer function is given by $\sin^2(\pi f)/(\pi f)^2$. Moreover, spatial averaging actually occurs over a volume rather than a line. If this volume is considered to be a right circular cylinder, then the analysis of Andreas (1981) implies that Equation (7) cannot be used when the diameter exceeds about 20% of the length.

3.2. Vector quantities

The effect of spatial averaging on measurements of the vector wind velocity components is different to that for scalar quantities. For a path length, p, both Kaimal *et al.* (1968) and Horst (1973) give the spectral transfer function, $T_i(k_1, p)$, for the wind component, u_i, as

$$T_i(k_1, p) = \frac{\displaystyle\iint_{-\infty}^{\infty} \frac{\sin^2(\mathbf{k}\cdot\mathbf{p}/2)}{(\mathbf{k}\cdot\mathbf{p}/2)^2}\,\Phi_{ii}(\mathbf{k})\,\mathrm{d}k_2\,\mathrm{d}k_3}{\displaystyle\iint_{-\infty}^{\infty} \Phi_{ii}(\mathbf{k})\,\mathrm{d}k_2\,\mathrm{d}k_3}\,, \tag{8}$$

where $\mathbf{k}$ is the wavennumber vector with components k_1, k_2, and k_3, $\mathbf{p}$ is the path vector and Φ_{ii} is the spectral density tensor. The transfer function, T_3 (or T_w) for the vertical wind velocity component is shown in Figure 2 plotted against the normalized frequency,

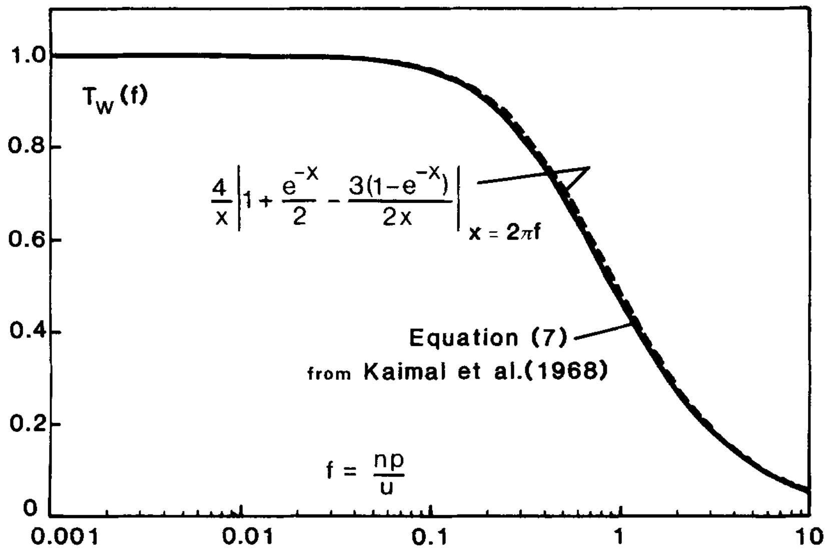

Fig. 2. Spectral transfer function, $T_w(f)$, associated with the measurement of vertical wind velocity averaged over a finite path length, p, shown as the solid curve plotted against normalized frequency $f = np/u$. The function approximating this curve is shown as a dashed line.

$f = np/u = k_1 p/2$. Again, a suitable expression representing T_w to an accuracy of better than 2% is also shown. It is suggested that the effective gain of a vertical wind component anemometer due to spatial averaging is adequately represented by

$$T_w(f) = \frac{2}{\pi f}\left(1 + \frac{e^{-2\pi f}}{2} - \frac{3(1 - e^{-2\pi f})}{4\pi f}\right) . \tag{9}$$

Generalized transfer functions for the horizontal wind velocity components are not possible, since they depend to a greater extent on instrument geometry and wind direction, as described in detail by Kaimal *et al.* (1968) and Horst (1973).

4. Sensor Separation

We consider the situation in which two identical sensors measure some atmospheric quantity represented by α at a spatial point P and α' at a second point P', while a third sensor measures a different quantity β at the first point P. The effect on measurement of turbulent flux associated with the correlation of quantities α and β due to separation of the two sensors by a distance, s, can be represented by a co-spectral transfer function, $T_s(n)$, defined as the ratio, $S_{\alpha'\beta}(n)/S_{\alpha\beta}(n)$, of the co-spectra of quantities α' and β and quantities α and β. To specify this transfer function, it is necessary to assume that it is equal to $S_{\alpha\alpha'}(n)/S_{\alpha\alpha}(n)$. This is arguably a reasonable assumption if α and β represent the vertical wind velocity component and some passive scalar quantity.

The co-spectrum of α and α' will depend on the angle between the separation path and the wind vector. If this path is parallel to the wind (i.e., longitudinal), then Taylor's frozen field hypothesis suggests that the two sensors will measure the same turbulent fluctuations, but there will be a phase shift between the two sets of measurements. If the separation is perpendicular (lateral) to the wind, then the fluctuations are different, but no phase shift is involved.

4.1. Lateral Separation

If lateral sensor separation is small and only affects the measured turbulent fluctuations in the inertial subrange, then Irwin (1979) and Kristensen and Jensen (1979) show that the co-spectral transfer function for the isotropic vertical wind velocity and scalar fields is given by

$$T_s(f) = \frac{2^{1/6}}{\Gamma(5/6)}(2\pi f)^{5/6} K_{5/6}(2\pi f). \tag{10}$$

Here, $f = ns/u$ with separation distance given by s, and $K_{5/6}$ is a modified Bessel function of the second kind. A plot of the transfer function is shown in Figure 3 where values of the weighted Bessel function were taken from Irwin (1979). Figure 3 also shows a plot of the function,

$$T_s(f) = e^{-9.9 f^{1.5}}, \tag{11}$$

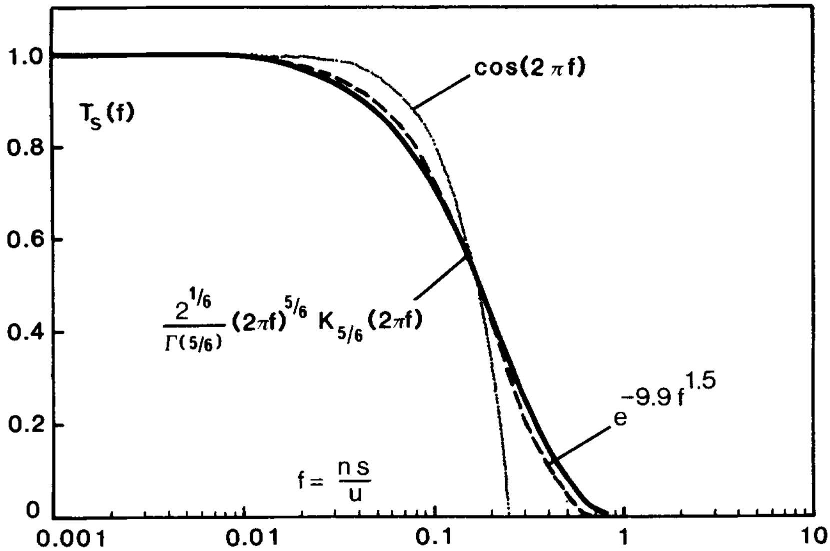

Fig. 3. Cospectral transfer function, $T_s(f)$, associated with the measurement of vertical wind velocity component at two positions separated laterally to the mean wind flow by a distance s, as shown by the solid curve plotted against normalized frequency $f = ns/u$. A function approximating this curve is shown as the dashed line.

which is considered to provide a good working description of the transfer function given by Equation (10). It can be seen from Figure 3, that only frequencies exceeding approximately $0.01u/s$ are affected by sensor separation. If Equation (10) is to be valid, such frequencies must be within the inertial subrange (representing isotropic turbulence), i.e., that $(0.01u/s) > n_i$, the frequency corresponding to the onset of local isotropy. Kaimal *et al.* (1972) indicate that for unstable conditions, $n_i > 0.1u/z$. Hence, as a rough guide, sensor separation should not exceed 10% of z, the height above zero-plane displacement, if it is not to influence non-isotropic turbulence. For stable conditions, Kaimal *et al.* found that $n_i > 1.4(z/L)(u/z)$, where L is the Obukhov length. In this case, sensor separation should be less than 0.7% of L, a condition which depends on atmospheric stability.

4.2. Longitudinal separation

Providing that s/u is small compared to the mean eddy lifetime, then longitudinal separation of sensors will introduce a phase shift related to s/u, in the cross-spectrum, $C_{\alpha\beta}(n)$, such that (Kristensen and Jensen, 1979),

$$C_{\alpha'\beta}(n) = e^{-2\pi jf} C_{\alpha\beta}(n) \ . \qquad (12)$$

Expanding Equation (12) gives

$$T_s(f) = \frac{S_{\alpha'\beta}(n)}{S_{\alpha\beta}(n)} = \cos(2\pi f) + \sin(2\pi f)\frac{Q_{\alpha\beta}(n)}{S_{\alpha\beta}(n)} \ . \qquad (13)$$

One method to account for the time delay associated with longitudinal separation may be to shift sample measurements digitally with time (this is necessary if air is drawn through an aspiration tube to a particular sensor). Alternatively, the quadrature spectrum, $Q_{\alpha\beta}(n)$, may be incorporated into a model accounting for the phase lag. In many situations, however, these methods are difficult to apply as the time delay will vary with wind speed and direction. Also, suitable descriptions of the quadrature spectra are not available.

Assuming that $Q_{\alpha\beta}(n)$ is small, a first approximation (cf. Hicks, 1972) is $T_s(f) = \cos(2\pi f)$ where $f = ns/u$ as before; this is plotted in Figure 3. As $\cos(2\pi f)$ decreases to zero, the quadrature term must become more significant, making this approximation invalid. However, inspection of Figure 3 indicates that $\cos(2\pi f)$ and the expression for lateral separation are not significantly different, with both functions having about the same 3 dB 'cut-off' frequency.

Hence, for the practical purpose of estimating flux loss from eddy-correlation systems consisting of sensors not widely separated and open to the atmosphere, it is suggested that Equation (11) be used for both lateral and longitudinal separation with the resulting simplification that corrections are independent of wind direction. This approach may lead to a small overestimate in flux loss, and should in any case be used with care.

5. Frequency Response of the Data Acquisition System

5.1. Sampling

Although many methods of data acquisition are available, analog to digital conversion is now the most common. If $x(t)$ and $y(t)$ represent two continuous signals being sampled at a rate of n_s, then the effective co-spectral transfer function, $T_a(n)$, is given by (e.g., Kaimal *et al.*, 1968),

$$T_a(n) = \begin{cases} 1 + \dfrac{\sum_{k=1}^{\infty} S_{xy}(kn_s - n) + S_{xy}(kn_s + n)}{S_{xy}(n)}, & n \leqslant n_s/2, \\ 0, & n > n_s/2; \end{cases} \tag{14}$$

where the summation term represents the effect of aliasing, or a folding of high-frequency co-spectral contributions about the Nyquist frequency, $n_s/2$. In practice, the effect of aliasing is minimized by first pre-filtering the signals $x(t)$ and $y(t)$ such that the co-spectrum, S_{xy}, has negligible power above the Nyquist frequency. For atmospheric measurements, such a co-spectrum may be approximated by a power law, Af^{-b} (Kristensen, 1974), where A is an arbitrary constant and b has a value probably between 2 and 5, but which depends on the type of pre-filter used. In this case, Equation (14) reduces to,

$$T_a = 1 + \left(\frac{n}{n_s - n}\right)^b, \quad n \leqslant n_s/2. \tag{15}$$

If expressions for the atmospheric spectra and co-spectra (see Section 6) and the response of the low-pass filter given by Equation (5) with $n_0 = n_s/2$, and $n_s = 10$ Hz are substituted in Equation (14), it can be shown that Equation (15) with $b = 3$ provides a description of the effect of aliasing to a good approximation.

5.2. Averaging

The process of separating a quantity into fluctuating and mean flow components defines the low frequency response of the eddy correlation technique. This is often accomplished by either taking block averages or linear detrends of stored data to obtain the mean, which is then subtracted from the original data to obtain the fluctuating component. In an analog system such as the Fluxation (Hicks, 1970), the mean is determined continuously by passing each signal through a simple low-pass RC filter having a gain function given by Equation (2) with a time constant τ = RC.

An equivalent process can be accomplished using a simple recursive low-pass digital filter, viz.,

$$\bar{q}_i = a\bar{q}_{i-1} + (1 - a)q_i \; , \tag{16}$$

where q_i represents the current measurement of q, while $\bar{q}_i$ and $\bar{q}_{i-1}$ represent the current and previous estimate of the mean. The parameter, a, is related to the time constant of the filter. With the development of inexpensive and powerful digital processors, filtering will increasingly be carried out using digital techniques. In particular, the technique provided by Equation (16) appears very suitable, being simple to apply and analyse. In addition, it can be shown, assuming Taylor's hypothesis, that it is similar to the process of taking instantaneous, unweighted spatial averages.

To obtain the fluctuation component, q', of quantity q for eddy-correlation analysis, it is usual to extract the mean component from the total quantity. From Equation (16),

$$q_i' = q_i - \bar{q}_i = a(q_i - q_{i-1}) + aq_{i-1}' \, . \tag{17}$$

This high-pass digital filter has a frequency response function, H_d, given by,

$$H_d = \frac{a(1 - e^{-2\pi jn/n_s})}{1 - a\,e^{-2\pi jn/n_s}} \; . \tag{18}$$

It can be shown that for frequencies smaller than the Nyquist frequency, the associated gain function, G_d, is given to a very good approximation by,

$$G_d(n) = \frac{2\pi n \tau_d}{\sqrt{1 + (2\pi n \tau_d)^2/a}} \; , \tag{19}$$

where the effective time constant is given by $\tau_d = a/((1 - a)n_s)$. If the time constant is large compared to the sampling period, then a has a value close to unity and Equation (19) represents the gain of a first-order high-pass filter similar to that for a simple RC filter.

6. Models of Atmospheric Spectra and Co-spectra

The most widely accepted descriptions of atmospheric spectra and co-spectra available in the literature have been developed from data collected during the Kansas and Minnesota boundary-layer experiments (Kaimal *et al.*, 1972, 1976). Such model spectra adopted for this paper have been modified for speed of computation and normalized to ensure that the computed integrals were equal to unity. Otherwise usual notation is used, where n represents frequency (Hz) and f is normalized frequency given by $f = nz/u$, z being the height above the zero-plane displacement and u the windspeed. Stability is represented by z/L, where L is Obukhov's length. Note that precision in the numerical constants does not represent precision in definition of the spectra, rather in the computational accuracy of the integral.

In this paper, the normalized spectra, $S_{\alpha\alpha}$ ($\alpha = T$, w, and u, i.e., of temperature, vertical, and horizontal wind velocity, respectively) for stable conditions ($z/L > 0$), are written in the form,

$$nS_{\alpha\alpha}(n) = \frac{f}{A_\alpha + B_\alpha f^{5/3}}, \tag{20a}$$

which can be derived from similar expressions given by Kaimal (1973). The quantities A_α and B_α are related to the peak spectral frequency, and are specified by,

$$A_T = 0.0961 + 0.644\left(\frac{z}{L}\right)^{0.6},$$

$$A_w = 0.838 + 1.172\left(\frac{z}{L}\right), \tag{20b}$$

and

$$A_u = 0.2A_w$$

with

$$B_\alpha = 3.124A_\alpha^{-2/3} \quad \text{for} \quad \alpha = T, w \text{ and } u.$$

Equations (20b) are determined from the peak frequency curves given by Kaimal *et al.* (1972). Similarly, normalized co-spectra, $S_{w\alpha}$ ($\alpha = T$ and u), for sensible heat and momentum are given by,

$$nS_{w\alpha}(n) = \frac{f}{A_{w\alpha} + B_{w\alpha} f^{2.1}}, \tag{21a}$$

where the quantities $A_{w\alpha}$ and $B_{w\alpha}$ are taken directly from Kaimal *et al.* (1972), viz.,

$$A_{wT} = 0.284\left(1 + 6.4\frac{z}{L}\right)^{0.75},$$

$$A_{uw} = 0.124\left(1 + 7.9\frac{z}{L}\right)^{0.75}, \tag{21b}$$

and

$$B_{w\alpha} = 2.34A_{w\alpha} \quad \text{for} \quad \alpha = T \text{ and } u.$$

Unfortunately, atmospheric spectra and co-spectra are not so easily described for unstable conditions ($z/L < 0$). It has been found (Kaimal *et al.*, 1976) that the non-isotropic low-frequency eddies do not obey Monin–Obukhov similarity and that the spectra contain convective and shear-driven contributions which in part, scale with the height of the boundary layer, z_i. However, Højstrup (1981) has described suitable models for the unstable vertical and horizontal wind velocity spectra which are written here in the form,

$$nS_{ww}(n) = \left(\frac{f}{1 + 5.3f^{5/3}} + \frac{16f\xi}{(1 + 17f)^{5/3}}\right) C_w^{-1} \tag{22}$$

and

$$nS_{uu}(n) = \left(\frac{210f}{(1 + 33f)^{5/3}} + \frac{f\xi}{\zeta + 2.2f^{5/3}}\right) C_u^{-1} \tag{23}$$

where

$$C_w = 0.7285 + 1.4115\xi, \qquad C_u = 9.546 + 1.235\xi\zeta^{-2/5}$$

with

$$\zeta = \left(\frac{z}{z_i}\right)^{5/3} \quad \text{and} \quad \xi = \left(\frac{z}{-L}\right)^{2/3}.$$

No suitable models describing the unstable atmospheric temperature spectrum, except for conditions of free convection (Panofsky, 1978), exist in the literature. In a recent study, Claussen (1985) produced a model that described many features of observed temperature spectra, but which was too complex for use here. However, this model showed that the low-frequency behaviour of the spectrum and its peak frequency varied little over a broad range of unstable conditions ($-z/L > 0.2$), a result in general agreement with the data of Kaimal *et al.* (1972). Only as neutral conditions were approached did significant shifts occur. Since variance in these conditions would be small, it was considered appropriate to use Equation (21d) in Kaimal *et al.* (1972) to describe the unstable temperature spectrum. The normalized version of this is given by,

$$nS_{TT}(n) = \begin{cases} \dfrac{14.94f}{(1 + 24f)^{5/3}} & f < 0.15, \\[2ex] \dfrac{6.827f}{(1 + 12.5f)^{5/3}} & f \geqslant 0.15. \end{cases} \tag{24}$$

Similarly, the low-frequency portion of the sensible heat and momentum cospectra cannot be defined precisely. The following expressions,

$$nS_{wT}(n) = \begin{cases} \dfrac{12.92f}{(1 + 26.7f)^{1.375}} & f < 0.54, \\[2ex] \dfrac{4.378f}{(1 + 3.8f)^{2.4}} & f \geqslant 0.54, \end{cases} \tag{25}$$

and

$$nS_{uw}(n) = \begin{cases} \dfrac{20.78f}{(1+31f)^{1.575}} & f < 0.24, \\ \dfrac{12.66f}{(1+9.6f)^{2.4}} & f \geqslant 0.24, \end{cases} \tag{26}$$

were determined as an average of the curves corresponding to the envelope of data over the range of stability from $z/L = 0$ to $z/L = -2$, as described in Kaimal *et al.* (1972). Typical errors incurred when estimating the frequency response correction resulting from this approach are described in Section 7.

Few experimental studies on the spectra and co-spectra of humidity and other scalars are available. However, the work of Redford *et al.* (1980), Smith and Anderson (1984), and Ohtaki (1985) provide evidence that such spectra are very similar to those for temperature. It was, therefore, assumed that the expressions derived for the temperature spectra and wT co-spectra could be applied to the humidity spectra and wq co-spectra, i.e.,

$$S_{qq} = S_{TT} \quad \text{and} \quad S_{wq} = S_{wT} . \tag{27}$$

7. Frequency Response Corrections

Within the limits of the simplifying assumptions made, the spectral transfer and response functions described in the previous sections can be applied to any eddy-correlation instrumentation. A typical system might consists of a sonic anemometer measuring the vertical wind velocity, w, a fast response sensor for measuring temperature, T, an absorption path hygrometer for measuring humidity, q, and an anemometer for measuring horizontal wind velocity, u. This system can be used for measuring the individual variances as well as sensible heat, H, latent heat, λE, and momentum flux, or equivalently, u_*^2. The transfer functions of such an arrangement would be given by

$$\begin{aligned} T_{TT}(n) &= T_d G^2(n, \tau_T) , \\ T_{qq}(n) &= T_d T_p(n, p_q) , \\ T_{ww}(n) &= T_d T_w(n, p_w) , \\ T_{uu}(n) &= T_d T_p(n, p_u) G^2(n, \tau_u) , \\ T_{wT}(n) &= T_d T_s(n, s_{wT}) G(n, \tau_T) \sqrt{T_w(n, p_w)} , \\ T_{wq}(n) &= T_d T_s(n, s_{wq}) \sqrt{T_w(n, p_w) T_p(n, p_q)} , \\ T_{uw}(n) &= T_d T_s(n, s_{uw}) G(n, \tau_u) \sqrt{T_w(n, p_w) T_p(n, p_u)} , \end{aligned} \tag{28}$$

where p_w, p_q, and p_u represent the averaging pathlengths of the w-anemometer, hygrometer, and u-anemometer; s_{wT}, s_{wq}, and s_{uw} the separation distances between the

w-, T-, q-, and u-sensors and τ_T and τ_u the time constants of the temperature sensor and u-anemometer, respectively. The transfer function of the data acquisition system, T_d is given by

$$T_d(n) = T_a(n, n_s)G_v^2(n, n_0)G_d^2(n, \tau_d),$$

where n_0 is the low-pass filter cut-off frequency, n_s is the sampling rate, and τ_d is the time constant of the high-pass digital filter. The set of expressions given by Equation (28) may be easily modified for alternative or additional system components.

7.1. Corrections for the Hydra System

The analysis described above has been used to define a frequency response correction procedure to be applied to flux and variance measurements made by the 'Hydra', an eddy-correlation system developed by the Institute of Hydrology. Such an analysis has shown that the arrangement of the prototype version of the Hydra could lead to significant flux loss in certain conditions, although in the case of measurements over tropical forest (cf. Shuttleworth *et al.*, 1984) such losses were small, in the order of 2 to 7% for sensible and latent heat and momentum fluxes. A new design of the Hydra has been developed with an improved performance and reduced frequency response loss.

This new Hydra includes a sonic anemometer (Shuttleworth *et al.*, 1982) with a path length of 20.0 cm for the measurement of w, a single (vertical) beam infra-red hygrometer (Moore, 1983) with a path length of 25.0 cm for the measurement of q-fluctuations, a fine-wire thermocouple of 40 μm diameter for the measurement of T, and a sensitive cup anemometer with rotor diameter of 15.2 cm and response length of 1.5 m for providing a measure of u_*. The separation distance of the hygrometer beam, thermocouple and cup anemometer rotor from the sonic anemometer path is 4.4, 6.5, and 52.6 cm, respectively.

Each of the signals from the Hydra sensors is passed through a 2-pole Butterworth filter (cf. Equation (5)) with a cut-off frequency of 5 Hz. These signals are multiplexed and digitized at a rate of 10 Hz by a CMOS microprocessor controlled data-acquisition and logging system similar to that described by Lloyd *et al.* (1984). The fluxes and variances were calculated on-line by effectively passing the individual signals through a high-pass digital recursive moving average filter of the type described in Section 5. This has a time constant of 18.75 min, equivalent to a value of a equal to 0.999 911 115.

Given these parameters, the transfer functions in Equations (28) were convoluted with the appropriate spectral and co-spectral expressions described in Section 6, and integrated as indicated by Equation (1). Transfer functions and spectra for certain conditions are illustrated in Figure 4. The integration scheme, implemented in BASIC on a microcomputer, consisted of first normalizing each logarithmic spectrum such that integration over the log-frequency range from −6 to 3 using Simpson's rule for 49 intervals, was unity. It was then found that integrating the reduced logarithmic spectrum to a sufficient accuracy (better than 1%) could be accomplished using Simpson's rule over 19 intervals in the log-frequency range −5 to log(5) (the upper limit corresponding

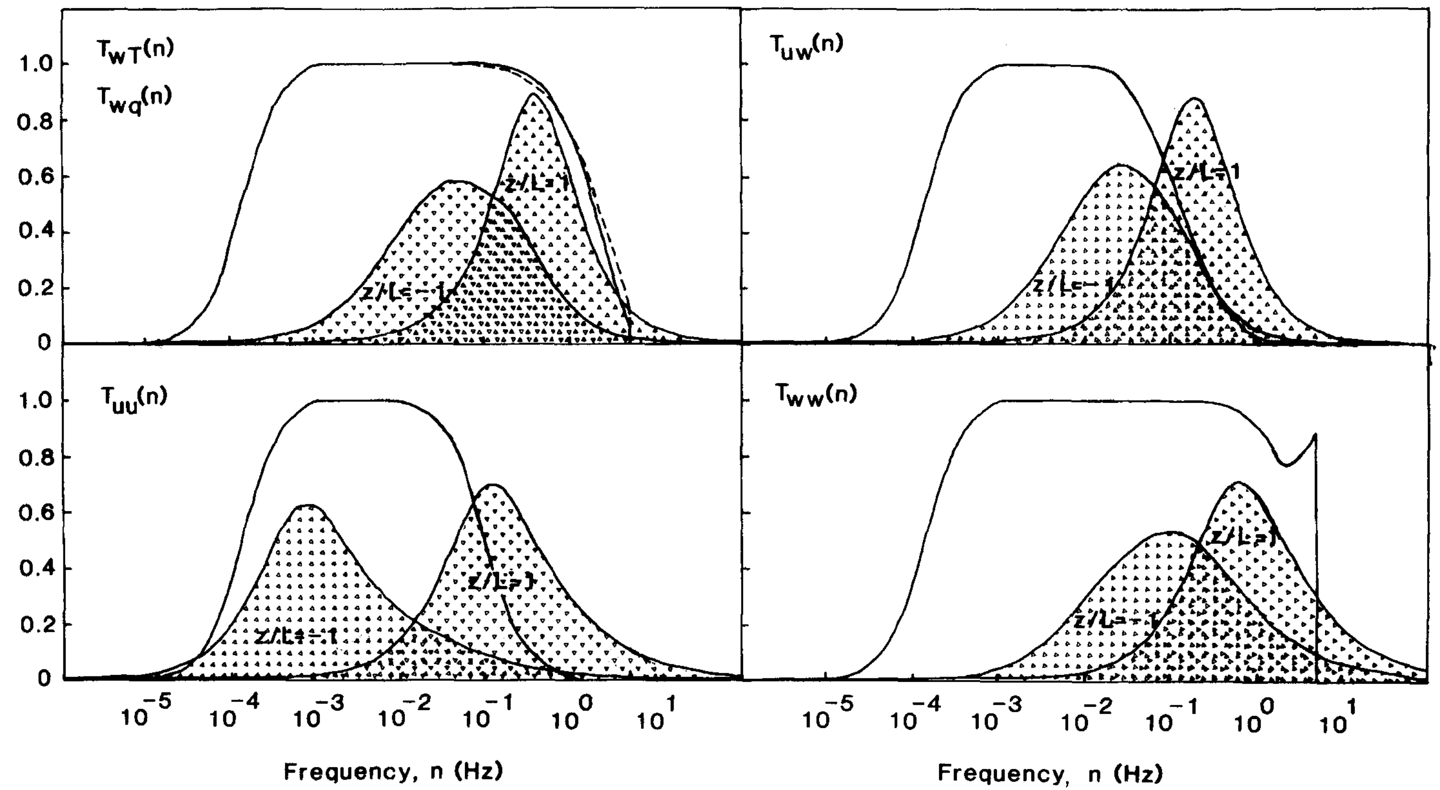

Fig. 4. Examples of the transfer functions for sensible heat (T_{wT}), latent heat (T_{wq}), and momentum (T_{uw}) fluxes and vertical (T_{ww}) and horizontal (T_{uu}) wind velocity variances. Curves are based on the Hydra eddy-correlation system mounted at a height of 2 m with a wind speed of 1 m s^{-1}. The relevant spectra and co-spectra for unstable ($z/L = -1$) and stable ($z/L = 1$) conditions are shown by the stipled areas plotted on an arbitrary scale.

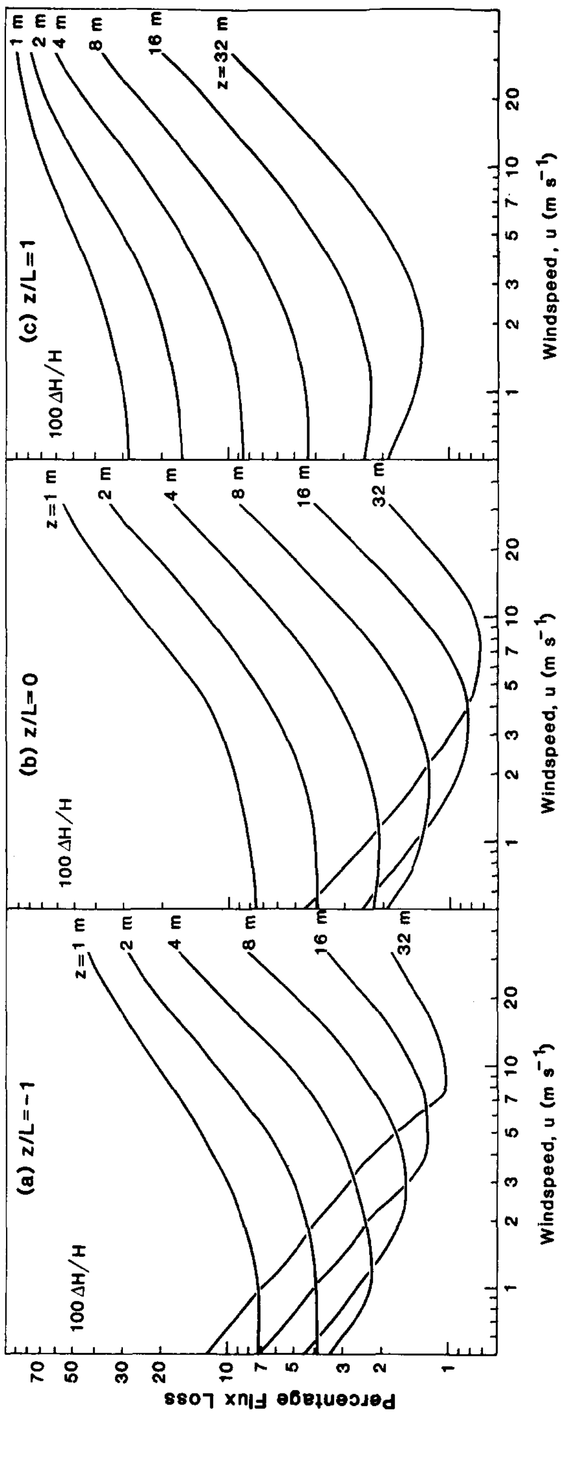

Fig. 5. Estimated percentage frequency response flux loss expected when measuring sensible heat flux in, (a) unstable ($z/L = -1$), (b) neutral ($z/L = 0$), and (c) stable ($z/L = 1$) conditions, using a Hydra eddy-correlation system with sensors installed at various heights, z, above the surface zero-plane displacement, and experiencing a range of wind speeds, u.

to the Nyquist frequency). In this way the computations took no longer than about 30 s for a given set of conditions on a CBM 64 microcomputer, although this was reduced to about 12 s if the program was first compiled.

Estimates of percentage sensible heat were thus calculated for a range of sensor heights from 1 to 32 m above zero-plane displacement and for a range of conditions including wind speed from 0.5 to 32 m s^{-1} and various stabilities. Figure (5) shows the results for (a) $z/L = -1$, (b) $z/L = 0$, and (c) $z/L = 1$. This procedure can be used to calculate losses from other fluxes. Estimates of latent heat flux loss were found to be similar to those of sensible heat.

If rapid calculation of the flux loss correction is required frequently, then it might be appropriate to fit some function to the calculated points; this can be accomplished to an accuracy of 20% or better over the range of values shown in Figure 5. However, determination of such a fitting function can be difficult and is only valid for a specific experimental situation. Although the integration scheme described above is not fast, it is accurate and more general, requiring only details of the eddy-correlation system, and estimates or measurements of height, windspeed and stability. The BASIC program developed for the Hydra is listed in the Appendix.

Although computational accuracy is high, over-all accuracy depends on the simplified expressions for the transfer functions and on the spectral models used. Further, uncertainty must also result from the inherent variability of the turbulent structure of the atmosphere; spectral models can only describe the mean behaviour. In addition, certain spectra used in the computation are not yet well understood. As mentioned in Section 6, the low-frequency components of the unstable co-spectra are not well defined, and in consequence an average spectral curve was used. The error in using this was determined by convoluting the transfer functions with curves corresponding to the inner ($-z/L > 0$) and outer ($-z/L < 2$) envelopes of the co-spectra given by Kaimal *et al.* (1972). The error in estimating sensible (or latent) heat flux percentage loss was found to be less than $\pm 3\%$ of the measured flux, or 26% of the estimated loss if this was greater. The error for momentum flux loss was less than $\pm 4\%$ of the flux, or if greater, 35% of the estimated loss. These values probably represent not only the errors in correcting unstable flux losses, but are also a realistic measure of the level of error involved in estimating loss corrections generally.

8. Conclusions

The eddy-correlation technique, being based on simple, fundamental physical principles, requires none of the simplifications or assumptions required by many other micro-meteorological techniques used for estimating atmospheric fluxes. However, it is impossible to design even a near-perfect sensor array required to implement the technique; compromise between sensor size and separation will always be necessary, while the bandwidth of sensors and data acquisition systems, although improving, will remain limited.

Fortunately, the response of the system components can be predicted fairly easily, while the consequences of sensor size and separation on measurements in isotropic turbulence can be understood and described, albeit in a complex way. This paper has shown that these descriptions can be greatly simplified for those conditions in which the eddy correlation technique will be of most practical use. This allows corrections for the amount of flux and variance lost due to frequency response to be estimated and routinely applied to eddy correlation measurements. Such corrections are typically less than 10%, but can be important and may account for up to 30% of measurements from some instrumental systems when atmospheric conditions are extreme or when exposure of sensors is not ideal.

The procedure for estimating frequency response corrections has been developed for use with the Institute of Hydrology's Hydra and is incorporated into the routine off-line analysis resulting in measurements of flux and variance. In this way, the contribution to measurement accuracy associated with frequency response loss is reduced to a remnant error in the order of $\pm 3\%$ or better.

Acknowledgements

I wish to thank my colleagues, W. J. Shuttleworth, J. H. C. Gash, and C. R. Lloyd at the Institute of Hydrology for their useful comments on this paper.

References

Andreas, E. L.: 1981, 'The Effects of Volume Averaging on Spectra Measured with a Lyman-Alpha Hygrometer', *J. Appl. Meteorol.* **20**, 467–475.

Campbell, G. S. and Unsworth, M. H.: 1979, 'An Inexpensive Sonic Anemometer for Eddy Correlation', *Boundary-Layer Meteorol.* **18**, 1072–1077.

Claussen, M.: 1985, 'A Model of Turbulence Spectra in the Atmospheric Surface Layer', *Boundary-Layer Meteorol.* **33**, 151–172.

Coppin, P. A. and Taylor, K. J.: 1983, 'A Three-Component Sonic Anemometer/Thermometer System for General Micrometeorological Research', *Boundary-Layer Meteorol.* **27**, 27–42.

Duchon, C. E.: 1963, 'The Infrared Radiation Temperature Correction for Spherical Temperature Sensors', *J. Appl. Meteorol.* **2**, 298–305.

Duchon, C. E.: 1964, 'Estimates of the Infrared Radiation Temperature Correction for Cylindrical Temperature Sensors', *J. Appl. Meteorol.* **3**, 327–335.

Garratt, J. R.: 1975, 'Limitations of the Eddy-Correlation Technique for the Determination of Turbulent Fluxes Near the Surface', *Boundary-Layer Meteorol.* **8**, 255–259.

Gurvich, A. S.: 1962, 'The Pulsation Spectra of the Vertical Component of Wind Velocity and Their Relations to the Micrometeorological Conditions', *Izv. Atmos. Oceanic Phys.* **4**, 101–136.

Hicks, B. B.: 1970, 'The Measurement of Atmospheric Fluxes Near the Surface: A Generalized Approach', *J. Appl. Meteorol.* **9**, 386–388.

Hicks, B. B.: 1972, 'Propellor Anemometers as Sensors of Atmospheric Turbulence', *Boundary-Layer Meteorol.* **3**, 214–228.

Højstrup, J.: 1981, 'A Simple Model for the Adjustment of Velocity Spectra in Unstable Conditions Downstream of an Abrupt Change in Roughness and Heat Flux', *Boundary-Layer Meteorol.* **21**, 341–356.

Højstrup, J., Rasmussen, K., and Larsen, S. E.: 1976, 'Dynamic Calibration of Temperature Wires in Still Air', *DISA Information*, No. 20, 22–29.

Horst, T. W.: 1973, 'Spectral Transfer Functions for a Three-Component Sonic Anemometer', *J. Appl. Meteorol.* **12**, 1072–1075.

Hyson, P. and Hicks, B. B.: 1975, 'A Single-Beam Infrared Hygrometer for Evaporation Measurement', *J. Appl. Meteorol.* **14**, 301–307.

Irwin, H. P. A. H.: 1979, 'Cross-Spectra of Turbulence Velocities in Isotropic Turbulence', *Boundary-Layer Meteorol.* **16**, 237–243.

Kaimal, J. C., Wyngaard, J. C., and Haugen, D. A.: 1968, 'Deriving Power Spectra from a Three-Component Sonic Anemometer', *J. Appl. Meteorol.* **7**, 827–834.

Kaimal, J. C., Wyngaard, J. C., Haugen, D. A., Cote, O. R., Izumi, Y., Caughey, S. J., and Readings, C. J.: 1976, 'Turbulence Structure in the Convective Boundary Layer', *J. Atmos. Sci.* **33**, 2152–2169.

Kaimal, J. C., Wyngaard, J. C., Izumi, Y., and Cote, O. R.: 1972, 'Spectral Characteristics of Surface Layer Turbulence', *Quart. J. R. Meteorol. Soc.* **98**, 563–589.

Kristensen, L.: 1974, 'Some Aspects olf the Application of Digital Techniques on Stochastic Time Series', *Danish A. E. C. Riso*, Report No. Riso-M-1756, 36 pp.

Kristensen, L. and Jensen, N. O.: 1979, 'Lateral Coherence in Isotropic Turbulence and in the Natural Wind', *Boundary-Layer Meteorol.* **17**, 353–373.

Larsen, S. E., Weller, F. W., and Businger, J. A.: 1979, 'A Phase Locked Loop Continuous Wave Sonic Anemometer Thermometer', *J. Appl. Meteorol.* **18**, 562–568.

Lloyd, C. R., Shuttleworth, W. J., Gash, J. H. C., and Turner, M.: 1984, 'A Microprocessor System for Eddy-Correlation', *Agr. For. Meteorol.* **33**, 67–80.

McBean, G. A.: 1972, 'Instrument Requirements for Eddy-Correlation Measurements', *J. Appl. Meteorol.* **11**, 1078–1084.

McNeil, D. D. and Shuttleworth, W. J.: 1975, 'Comparative Measurements of the Energy Fluxes over a Pine Forest', *Boundary-Layer Meteorol.* **9**, 297–313.

Moore, C. J.: 1976, Eddy Flux Measurements Above a Pine Forest', *Quart. J. Roy. Meteorol. Soc.* **102**, 913–918.

Moore, C. J.: 1983, On the Calibration and Temperature Behaviour of Single-Beam Infrared Hygrometers', *Boundary-Layer Meteorol.* **25**, 245–269.

Ohtaki, E.: 1984, 'Application of an Infrared Carbon Dioxide and Humidity Instrument to Studies Turbulent Transport', *Boundary-Layer Meteorol.* **29**, 85–107.

Ohtaki, E.: 1985, 'On the Similarity in Atmospheric Fluctuations of Carbon Dioxide, Water Vapour and Temperature over Vegetated Fields', *Boundary-Layer Meteorol.* **32**, 25–37.

Panofsky, H. A.: 1978, 'Matching in the Convective Planetary Boundary Layer', *J. Atmos. Sci.* **35**, 272–276.

Raupach, M. R.: 1978, 'Infrared Fluctuation Hygrometry in the Atmospheric Surface Layer', *Quart. J. R. Meteorol. Soc.* **104**, 309–322.

Redford, T. G., Jr., Verma, S. B., and Rosenberg, N. J.: 1980, 'Humidity Fluctuations over a Vegetated Surface Measured with a Lyman-Alpha Hygrometer and a Fine-Wire Thermocouple Psychrometer', *J. Appl. Meteorol.* **19**, 860–867.

Shuttleworth, W. J., Gash, J. H. C., Lloyd, C. R., Moore, C. J., Roberts, J., Marques, A., Fish, G., Silva, V., Nazare, M., Molion, L. C. B., Abreu Sa, L., Nobre, C. A., Cabral, O. M. R., Patel, S. R., and Carvalho, J.: 1984, 'Eddy-Correlation Measurements of Energy Partition for Amazonian Forest', *Quart. J. R. Meteorol. Soc.* **110**, 1143–1162.

Shuttleworth, W. J., McNeil, D. D., and Moore, C. J.: 1982, 'A Switched Continuous-Wave Sonic Anemometer for Measuring Surface Heat Fluxes', *Boundary-Layer Meteorol.* **23**, 425–448.

Silverman, B. A.: 1968, 'The Effect of Spatial Averaging on Spectrum Estimation', *J. Appl. Meteorol.* **7**, 168–172.

Smith, S. D. and Anderson, R. J.: 1984, 'Spectra of Humidity, Temperature, and Wind over the Sea at Sable Island, Nova Scotia', *J. Geophys. Res.* **89**, 2029–2040.

Spittlehouse, D. L. and Black, T. A.: 1979, 'Determination of Forest Evapotranspiration Using Bowen Ratio and Eddy-Correlation Measurements', *J. Appl. Meteorol.* **18**, 647–653.

Appendix

Listing of a microcomputer BASIC program for calculation of the frequency response corrections required for atmospheric flux and variance measurements using an eddy-correlation system.

```
100 REM ★★★★★★★★★★★★★★★★★★★★★★★★★★★★★★★★★★★★★★★★★★★★★★★★★★★★★★★★★★
110 REM ★ THIS PROGRAM DETERMINES FREQUENCY RESPONSE LOSS FROM MEASUREMENTS   ★
120 REM ★ OF TURBULENT FLUXES AND VARIANCES USING AN EDDY CORRELATION SYSTEM. ★
130 REM ★ GAIN/TRANSFER FUNCTIONS, G1-G7, ARE CALCULATED IN LINES 580-670, AND ★
140 REM ★ CONVOLUTED WITH RELEVANT ATMOSPHERIC SPECTRA OR CO-SPECTRA CALCULATED ★
150 REM ★ IN LINES 670-740. MEASURED FLUXES AND VARIANCES CAN BE ADJUSTED BY   ★
160 REM ★ MULTIPLYING WITH THE RESULTING CORRECTION FACTORS, S1-S7.            ★
170 REM ★                                                                      ★
180 REM ★ THE FOLLOWING QUANTITIES NEED TO BE SPECIFIED:                       ★
190 REM ★     Z  = HEIGHT ABOVE ZERO-PLANE DISPLACEMENT                        ★
200 REM ★     U  = WIND SPEED AT HEIGHT Z                                      ★
210 REM ★     ZL = Z/L THE MONIN-OBUKHOV STABILITY PARAMETER                   ★
220 REM ★                                                                      ★
230 REM ★     D1 = THERMOMETER TIME CONSTANT AT ZERO WIND (U=0)     (SECONDS)  ★
240 REM ★     D2 = RESPONSE LENGTH OF CUP OR PROPELLOR ANEMOMETER   (METRES)   ★
250 REM ★     D3 = TIME CONSTANT OF LOW-PASS BUTTERWORTH FILTER     (SECONDS)  ★
260 REM ★     PQ = PATH LENGTH OF Q-SENSOR  (METRES)                           ★
270 REM ★     PW = PATH LENGTH OF W-SENSOR  (METRES)                           ★
280 REM ★     PU = PATH LENGTH OF U-SENSOR  (METRES)                           ★
290 REM ★     XT = SEPARATION OF W AND T SENSORS  (METRES)                     ★
300 REM ★     XQ = SEPARATION OF W AND Q SENSORS  (METRES)                     ★
310 REM ★     XU = SEPARATION OF W AND U SENSORS  (METRES)                     ★
320 REM ★     DC = TIME CONSTANT OF DIGITAL HIGH-PASS FILTER  (SECONDS)        ★
330 REM ★     NS = SAMPLING FREQUENCY                  (HZ)                    ★
340 REM ★                                                                      ★
350 REM ★ THE VARIABLES USED FOR THE SPECTRA, TRANSFER FUNCTIONS AND           ★
360 REM ★ CORRECTION FACTORS ARE:                                              ★
370 REM ★ CORRELATION  (CO)SPECTRUM  TRANSFER FUNCTION  CORRECTION FACTOR      ★
380 REM ★    W-T           WT              G1                  S1              ★
390 REM ★    W-Q           WT              G2                  S2              ★
400 REM ★    U-W           UW              G3                  S3              ★
410 REM ★    T-T           TT              G4                  S4              ★
420 REM ★    Q-Q           TT              G5                  S5              ★
430 REM ★    U-U           UU              G6                  S6              ★
440 REM ★    W-W           WW              G7                  S7              ★
450 REM ★★★★★★★★★★★★★★★★★★★★★★★★★★★★★★★★★★★★★★★★★★★★★★★★★★★★★★★★★★
460 GOSUB510:I3=0:FORI1=1TO10:FORI2=2TO4STEP2:I3=I3+1:IFI3>19THEN500
470 I4=I2+(I3=1)+(I3=19):GOSUB580
480 S1=S1+I4*G1*WT:S2=S2+I4*G2*WT:S3=S3+I4*G3*UW:S4=S4+I4*G4*TT
490 S5=S5+I4*G5*TT:S6=S6+I4*G6*UU:S7=S7+I4*G7*WW:N=N*LF
500 NEXT:NEXT:S1=C/S1:S2=C/S2:S3=C/S3:S4:S5=C/S5:S6=C/S6:S7=C/57:RETURN
510 TC=D1/(1+4.9*(SQR(D1)*U)^0.45):TC=TC*TC:UC=D2/U:UC=UC*UC:VC=D3*D3:C=4.115
520 S1=0:S2=0:S3=0:S4=0:S5=0:S6=0:S7=0:N=1E-5:LF=2.073:B=1.667:IFZL>=0THEN550
530 X1=(-ZL)^0.667:X2=(0.001*Z)^B:CW=0.7285+1.4115*X1
540 CU=9.546+1.235*X1/(X2^0.4):RETURN
550 X1=0.284*(1+6.3*ZL)^0.75:X2=0.124*(1+7.9*ZL)^0.75:X3=0.0961+0.644*ZL^0.6
560 X4=0.838+1.172*ZL:X5=0.2*X4:Y1=2.34/X1^1.1:Y2=2.34/X2^1.1
570 Y3=3.124/X3^0.667:Y4=3.124/X4^0.667:Y5=3.124/X5^0.667:RETURN
580 IFN>NS/2THENG1=0:G2=0:G3=0:G4=0:G5=0:G6=0:G7=0:RETURN
590 W=6.283*N:NU=N/U:WU=W/U:W2=W*W:GD=1:X=W*DC:IFX<6THENX=X*X:GD=X/(1+X)
600 TR=1+W2*TC:QP=1:X=WU*PQ:IFX>0.02THENY=EXP(-X):QP=3+Y-4*(1-Y)/X:QP=QP/X
610 UR=1+W2*UC:UP=1:X=WU*PU:IFX>0.02THENY=EXP(-X):UP=3+Y-4*(1-Y)/X:UP=UP/X
620 GV=W2*VC:WP=1:X=WU*PW:IFX>0.04THENY=EXP(-X):WP=1+(Y-3*(1-Y)/X)/2:WP=4*WP/X
630 GV=1+GV*GV:TS=1:X=NU*XT:IFX>0.01THENTS=EXP(-9.9*X^1.5)
640 X=N/(NS-N):GA=1+X*X*X:QS=1:X=NU*XQ:IFX>0.01THENQS=EXP(-9.9*X^1.5)
650 GX=GA*GD/GV:US=1:X=NU*XU:IFX>0.01THENUS=EXP(-9.9*X^1.5)
660 G1=GX*TS*SQR(WP/TR):G2=GD*GX*QS*SQR(WP*QP):G3=GX*US*SQR(WP*UP/UR)
670 G4=GX/TR:G5=GD*GX*QP:G6=GX*UP/UR:G7=GX*WP
680 F=NU*Z:F1=F^B:IFZL<0THEN710
690 F2=F^2.1:WT=F/(X1+Y1*F2):UW=F/(X2+Y2*F2):TT=F/(X3+Y3*F1)
700 WW=F/(X4+Y4*F1):UU=F/(X5+Y5*F1):RETURN
710 WW=16*F*X1/(1+17*F)^B:IFF>=0.54THENWT=4.378*F/(+3.8*F)^2.4
720 WW=WW+F/(1+5.3*F1):IFF<0.54THENWT=12.92*F/(1+26.7*F)^1.375
730 IFF>=0.2THENUW=12.66*F/(1+9.6*F)^2.4:TT=6.827*F/(1+12.5*F)^B
740 IFF<0.2THENUW=20.78*F/(1+31*F)^1.575:TT=14.94*F/(1+24*F)^B
750 UU=210*F(1+33*F)^B+F*X1/(X2+2.2*F1):UU=UU/CU:WW=WW/CW:RETURN
```